[1] M. Karthikraja*

[2] Dr. P. Kalidoss

[3] Dr. S. Anbu

Innovating Sustainable Turning Processes: Exploring Improved Thermal Performance with Computational Fluid Dynamics Simulations of Cu/Al2O3/MWCNT Nanocoolants

JES
Journal of Electrical Systems

Abstract: - This study plans to mathematically research the warm presentation of cutting liquids scattered with nanoparticles for proficient intensity evacuation during turning tasks. Ansys Familiar programming is used for recreations, utilizing a three-layered fierce incompressible single- stage stream to display the issue. The computational space incorporates a warmed cutting instrument and workpiece, with nanocoolants splashed from a spout over the machining zone. Mineral oil is blended in with nanoparticles of MWCNT (multi-walled carbon nanotube), Cu (copper), and Al_2O_3 (aluminium oxide) to make nanocoolants. By changing the coolant speed (Uc) and nanoparticle volume portion (φ) inside the scope of 2% ≤ φ ≥ 8% and 1 m/s ≤ Uc ≥ 20 m/s, individually, the intensity move capacities of different nanocoolants are looked at. The discoveries uncover that rising coolant speed and the volume part of scattered nanoparticles prompts a huge drop in the cutting device's temperature. The typical cutting apparatus temperature diminishes by 25.65%, while the typical intensity moves rate increments by 25.43% with expanding volume portion. Furthermore, MWCNT nanocoolants exhibit prevalent warm execution and intensity expulsion rate contrasted with Cu and Al2O3 nanocoolants. The dissected mathematical outcomes are approved and adjust well to the benchmark results approved in the writing.

Keywords: nanocoolant, cutting temperature, cutting fluid velocity, multi wall carbon nanotubes.

I. INTRODUCTION

Various ventures utilize testing to-cut materials, for example, titanium and nickel-based compounds in machining processes. The extreme intensity produced during machining tasks abbreviates the cutting apparatus' life expectancy. Cutting liquids are fundamental in machining to dispense with chips from the apparatus and workpiece contact, as well as to give cooling and oil. Considering that device temperature essentially influences its life expectancy, cutting liquid is showered at the apparatus workpiece point of interaction to keep up with the instrument at an ideal temperature. Penetrating, turning, and processing cycles can all profit from the utilization of nanocoolants to upgrade cooling execution all through machining. Nanocoolants, by consolidating nanoparticles into the cutting liquid, can disperse heat all the more quickly, show fundamentally higher warm conductivity, and draw out the cutting device's life. Further developed cooling and oil from cutting liquids can altogether improve machining effectiveness. In high-temperature conditions, the base oil framework may not be such cases, scattering nanoparticles in the fundamental coolant upgrades its tribological qualities and warm conductivity. Anandan et al. [1] directed a trial concentrate on turning AISI M42 steel utilizing graphene nanofluids, which uncovered a critical temperature decrease contrasted with oil and dry circumstances with negligible oil. The temperature diminished by 67% contrasted with oil and by 72% in a climate with negligible grease. Contrasted with dry machining, the consideration of nanofluid brought about an 85% decrease in surface harshness, a 72% temperature decrease, and a 93% lessening in clear wear. In the examination by Buddy et al. [2], sunflower oil was utilized as the base liquid in a negligible sum grease approach Al_2O_3 nanoparticles were then added to the blend. Hardened steel AISI 321 was bored utilizing the subsequent colloidal scattering. The review inspected drill tip temperature, surface unpleasantness, boring powers, and device wear of hardened steel under different cooling plans. Also, they observed that unfortunate boring quality was the aftereffect of dry penetrating. Boring powers, including force and push force, were generally diminished to 83% and 42%, separately, contrasted with those during flood penetrating on account of 3.5 weight percent nanofluid with least oil conditions. Al_2O_3 nanoparticles fundamentally affect upgrading the greasing up and cooling characteristics of vegetable-based cutting liquids and further developing

[1] Dhanalakshmi Srinivasan University, Tiruchirappalli, Tamil Nadu, India. karthikmechmo@gmail.com

[2] Dhanalakshmi Srinivasan University, Tiruchirappalli, Tamil Nadu, India. kalidossp.set@dsuniversity.ac.in

[3] Dhanalakshmi Srinivasan Engineering College, Perambalur, Tamil Nadu, India. sathasivamanbu1974@gmail.com

* Corresponding Author Email: karthikmechmo@gmail.com

penetrating qualities connected with drill tip temperature. Moreover, when contrasted with dry and flood conditions, nanofluid negligible sum grease essentially diminish the force of grip on the instrument. When turning hardened steel with a tungsten tool, Gajrani et al. [3] used calcium disulphide and molybdenum disulphide. 11.01% less tool chip contact friction was found as a consequence. Singh et al. [4] directed probes surface crushing of Ti6Al4V-ELI composite utilizing a cubic boron nitride crushing haggle the tribological execution of three unmistakable nanoparticles - graphene, graphite, and MoS2 scattered in canola, soybean, and olive vegetable oils. They accomplished agreeable crushing execution utilizing the manufactured liquid based insignificant amount oil. Various hybrid nanoparticle combinations (MoS2/WS2, WS2/hBN, and MoS2/hBN) were used by Kumar et al. [5] to grind silicon nitride. It is possible to notice that the silicon nitride workpiece's surface roughness decreased together with its chipping layer's depth. When grinding titanium alloy using MQL, Setti et al. [6] tested with varying the volume concentration of alumina and copper oxide nanoparticles in water at 0.05, 0.1, 0.5, and 1%. Employing the nanofluids is claimed to lower the grinding temperature and tangential force. Tooth et al. [7] conceived a clever cooling channel to expand instrument life and found that rising coolant tension can improve machining execution and lessen wear obstruction.The tribofilm formed on the machined surface was made possible by the increased quantity of nanoparticles. They accomplished agreeable crushing execution utilizing the manufactured liquid based insignificant amount oil. Jerold et al. [8] used cryogenic CO_2 as a slicing liquid during going cycles to machine AISI 1045 steel. The use of cryogenic coolants brought about a decrease of the slicing temperature by 7% to 24% as per the outcomes. This abatement in slicing temperature was displayed to draw out apparatus life and improve surface quality and chip fragility. They likewise saw that cryogenic machining brought down the slicing force by 19% to 39%. Also, they recommended utilizing cryogenic CO_2 rather than conventional coolants gave natural circumstances are all around checked during cryogenic processing. Molybdenum disulphide and carbon nanotube hybrid nanoparticles were used in Zhang et al.'s [9] grinding process for nickel alloy. When compared to single nanofluid, hybrid nanofluid demonstrated superior lubrication, according to the experimental results. Suaib et al [10].Furthermore, studies have shown that raising the Reynolds number, channel aspect ratio, and concentration of nanoparticles can result in decreased maximum temperatures in cooling channels and improved heat transfer, suggesting the possibility for better thermal performance in heat dissipation applications. Zhang and colleagues [11] used a minimal amount of lubrication to grind an alloy based on nickel utilizing several nanoparticles, including MoS2-CNTs and MoS2-CNTs. The use of hybrid molybdenum disulphide and carbon nanotube nanoparticles resulted in a lower grinding force ratio and surface roughness. Titanium alloy was machined in an experiment by Jamil et al. [12] utilizing a hybrid nanofluid of carbon nanotube and alumina mixed together. The effectiveness of cryogenic cooling and MQL machining were compared. When using hybrid nanofluid for machining, the results indicated an 8.72% drop in surface roughness and an 11.8% decrease in cutting force. The tribofilm formed on the machined surface was made possible by the increased quantity of nanoparticles. Hard turning of chromium steel was achieved by Duc et al. [13] using alumina and molybdenum disulphide together. Heat conductivity and lubricating characteristics both improved, according to the trial. Due to the fact that hybrid nanofluids create a strong film at the contacting surfaces, which lowers friction and thus lowers cutting forces, Gugulothu and Pasam [14] examined the efficiency of employing hybrid nanofluids in cutting force reduction when compared to dry machining. Additionally, cutting forces and friction are decreased by the hybrid nanofluids' synergistic impact. On hardened steel, Jia et al. [15] carried out MQL and dry grinding. Lower specific grinding energy was achieved using MQL grinding as compared to dry grinding. When grinding titanium alloy using MQL, Das et al. [3] led a review utilizing four unmistakable nanoparticles - CuO, ZnO, Al_2O_3, and Fe_2O_3 in deionized water to survey cutting execution and lead a relative assessment pointed toward further developing machinability during the hard-turning activity composite AISI 4340 prepares utilizing the base amount oil strategy. The outcomes demonstrate a critical improvement in the work_piece's surface quality while changing from Al_2O_3 to CuO nanofluid. The CuO base nanofluid has lower thickness than ZnO, Al_2O_3, Fe_2O_3 nanofluids, adding to upgraded surface clean. This likewise works with the fitting settling of the nanofluid at the connection point between the workpiece and the device, making a padding impact that lessens babbling and vibrations during cutting. Alumina and silicon carbide nanoparticles of sizes of 30, 50, and 70 nm, respectively, were hybridized to grind nickel alloy, as reported by Zhang et al. [17]. Yi et al's. Study [18] dove into the way of behaving of graphene oxide nanofluids during the turning of Ti-6Al-4V. They explored different perspectives like surface harshness, chip arrangement, and cutting temperature. Bouri et al. [19] completed a trial examination to inspect the temperature profile close to the cutting locale. They contrasted spray water with MQL and saw that spray water displayed a higher pace of intensity move and temperature decrease.

Broad exploration has been directed on apparatus wear in turning applications, including an assessment of the effect of cutting liquid. Furthermore, they referenced [20] that typical cutting liquids can be supplanted with 10% vegetable emulsifier oil. Sharma et al. [21] led an exhaustive survey and examination of different grease methodologies, including high-pressure pooling, cryogenic cooling, packed cooling, close dry machining, and insignificant amount oil. Gariani et al. [22] introduced an itemized investigation of a remarkable cutting liquid impingement conveyance framework intended to limit the utilization of cutting liquid. They accomplished a by and large 42% decreases in cutting liquid and actually diminished device flank wear by 46.77%. Nanofluids were proposed as choices by Srikant et al. [23], basically for insignificant amount oil. They showed that nanofluids enjoy an upper hand over different liquids because of their improved warm conductivity, making them reasonable for the machining area. Cutting force, surface roughness, and wear were assessed by Zenjanab et al. [24] utilizing CuO and boric acid nanoparticles in a hybrid nanofluid environment on AISI 4340 steel with a cermet carbide insert. Applying nanofluids resulted in a 31% and 59% decrease in cutting force and surface roughness. This decrease may be ascribed to the boric acid nanoparticle additions' lubricating quality, which greatly reduced friction. The variation over the cutting tool was predicted by Sharma et al. [25] using computational fluid dynamics and alumina-multiwalled carbon nanotube. Reduced cutting forces and enhanced heat conductivity were shown via hybrid nanofluid. This study expects to analyze and look at the warm exhibition of various nanocoolants, including mineral oil coolant regularly utilized in turning tasks, Al_2O_3, Cu, and Multi-Wall Carbon Nanotube (MWCNT) nanoparticles. It mathematically explores the temperature dispersion on the cutting instrument and workpiece surface for these different nanocoolants during turning activities utilizing Computational Liquid Elements (CFD). The workpiece and device in the computational space are warmed, and a spout over the machining zone is used to shower nanocoolants. Parametric examinations include changing the nanocoolant speed and nanoparticle volume rate. The results are examined by assessing the stream and intensity move properties close to the machining zone. Further examinations include plotting temperature shapes, greatest cutting temperature, wall heat move coefficient, and Nusselt number.

II. EQUATIONS

2.1 Problem Statement and Physical Constraints

The issue is formed as a three-layered tempestuous incompressible stream. Nanocoolants are scattered into the machining zone by means of a 6-mm breadth spout.
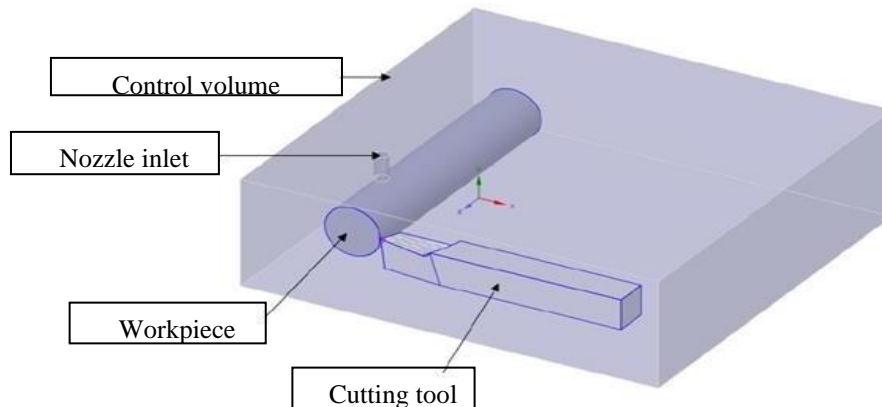

Figure.1 Computational area containing cutting apparatus

Continuity equation:

$$\frac{\partial(\rho_m)}{\partial t} + \nabla \cdot \left(\rho_m \vec{V}_m\right) = 0 \tag{1}$$

Momentum equation:

$$\partial \left(\frac{\rho_m \vec{V}_m}{\partial t} + \nabla \cdot \left(\rho_m \vec{V}_m \vec{V}_m\right)\right) = -\nabla P_m + \nabla \cdot \left[\mu_m \left(\nabla \vec{V}_m + \overrightarrow{V_m^T}\right)\right] - \rho_m \beta_m g(T_h - T_c) \tag{2}$$

Energy equation:

$$\frac{\partial(\rho_m C_{pm} T_m)}{\partial t} + \nabla \cdot \left(\rho_m C_{pm} T_m \overrightarrow{V_m}\right) = \nabla \cdot [k_m(\nabla T_m)] \tag{3}$$

Turbulence Model:

The following are the SST k-ω model equations

$$\frac{\partial(\rho_m k)}{\partial t} + \frac{\partial}{\partial x_i}\left(\rho_m \overrightarrow{\mathcal{V}_m}\mathrm{k}\right) = \frac{\partial}{\partial x_j}\left[\Gamma_k \frac{\partial k}{\partial x_j}\right] + G_k - Y_k + S_k \qquad (4)$$

$$\frac{\partial(\rho_m \omega)}{\partial t} + \frac{\partial}{\partial x_j}\left(\rho_m \vec{\mathcal{V}}_m \omega\right) = \frac{\partial}{\partial x_j}\left[\Gamma_\omega \frac{\partial \omega}{\partial x_j}\right] + G_\omega - Y_\omega + D_\omega + S_\omega \qquad (5)$$

$$D_\omega = 2\,(1 - F_1)\,\rho\,\sigma_\omega,\ 2\,\frac{1}{\omega}\frac{\partial k}{\partial x_j}\frac{\partial \omega}{\partial x_j} \qquad (6)$$

The Reynolds number and Nusselt number may be calculated by utilizing Equation (7) and (8) accordingly

$$Re = \frac{\rho_m V_m D}{\mu_m} \qquad (7)$$

$$Nu = \frac{hl}{k_m} \qquad (8)$$

The symbols D and l are used to denote the diameter that defines the nozzle and the standard length of the tool's tip respectively.

2.2 Overseeing Conditions

The cutting liquid is formed as mineral oil joined with aluminum oxide, copper particles, and multi-walled carbon nanotubes. It is accepted that the nanoparticles are round and mono-scattered. The following are the administering conditions for scattering rate, energy, energy, progression, and tempestuous dynamic energy.

III. IMPLEMENTATION METHOD

3.1 Choice of Appropriate Nanoparticles Thermophysical Properties of Nanofluid

Table's 1-4 rundown the thermophysical attributes of the base liquid mineral oil and a few nanoparticles utilized in this work, including Cu, Al$_2$O$_3$, and MWCNT.

Table.1 Thermophysical also, mechanical properties of nanoparticles

Nanoparticle	Thermal Conductivity (W/m-K)	Specific Heat (J/kg-K)	Density (kg/m^3)
Al$_2$O$_3$	36.6	752	3910
MWCNT	3000	550	1500
Cu	398	390	8850

Table.2 Thermophysical and mechanical properties of mineral oil scattered with Al$_2$O$_3$

Cutting Fluid	Thermal Conductivity (W/m-K)	Density (kg/m^3)	Dynamic Viscosity (kg/m-s)	Specific Heat (J/kg-K)
BASEFLUID- Mineral Oil	0.1335	856.5	0.06380925	1918
Mineral Oil + Al$_2$O$_3$ (2%)	0.143464	931.44	0.073245	1895.04
Mineral Oil + Al$_2$O$_3$ (4%)	0.150634	986.84	0.084353	1874.63
Mineral Oil + Al$_2$O$_3$ (6%)	0.156454	1042.64	0.090745	1845.85
Mineral Oil + Al$_2$O$_3$ (8%)	0.166457	1121.64	0.098745	1827.75

$$\rho m = (1 - \phi)\rho bf + \phi \rho np \qquad (9)$$

The warm diffusivity of the nanofluid is given by:

$$\alpha m = km/(\rho cp)m \tag{10}$$

Where (ρcp) signifies the intensity capacitance of the nanofluid

$$(\rho cp)m = (1 - \phi)(\rho cp)bf + \phi(\rho)np \tag{11}$$

The mathematical portrayal of thermophysical property estimations for the Cu focus range is   seen as in Table 4 and is likewise utilized in these reproductions.

Table.3 Thermophysical mechanical properties of mineral oil scattered with MWCNT

CuttingFluid	Thermal Conductivity (W/m-K)	Density (kg/m³)	Dynamic_Viscosity (kg/m-s)	Specific Heat (J/kg-K)
BASEFLUID-Mineral Oil	0.1335	856.5	0.06380925	1918
Mineral Oil + MWCNT (2%)	0.148668	893.64	0.070686	1887.77
Mineral Oil + MWCNT (4%)	0.1556575	937.76	0.077567	1860.65
Mineral Oil + MWCNT (6%)	0.1596765	974.55	0.0827575	1830.75
Mineral Oil + MWCNT (8%)	0.1686457	998.67	0.097976	1796.76

Table.4 Thermophysical & mechanical properties of mineral oil scattered with Cu

Cutting Fluid	Thermal Conductivity (W/m-K)	Density (kg/m³)	Dynamic Viscosity (kg/m-s)	Specific Heat (J/kg-K)
BASEFLUID-Mineral Oil	0.1335	856.5	0.06380925	1918
Mineral Oil + Cu (2%)	0.146466	895.75	0.070454	1899.55
Mineral Oil + Cu (4%)	0.153243	934.65	0.076464	1873.34
Mineral Oil + Cu (6%)	0.159566	974.78	0.083636	1852.78
Mineral Oil + Cu (8%)	0.169968	1007	0.090576	1831.67

3.2 Independence Study of Mesh

To relieve the downsides of the regular technique, the lattice count is differed from coarser to better work until there is negligible temperature variety concerning the cross section count. The lattice count is iterated with 12 different cross section counts beginning from 3.86 million cross section components, bringing about a 0.57% temperature variety. In this way, the cross section is refined to a better level, bringing about a 3.48 million lattice count and a 0.32% temperature variety, which is thought of as satisfactory.
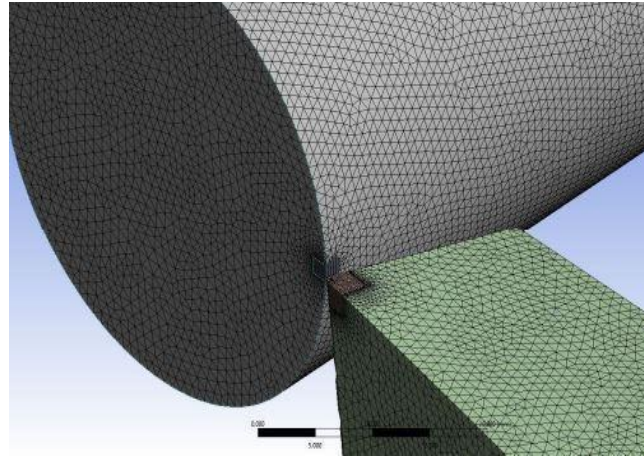
Figure.2 Coincided cutting instrument and work piece lattice count of 3.86 million cells
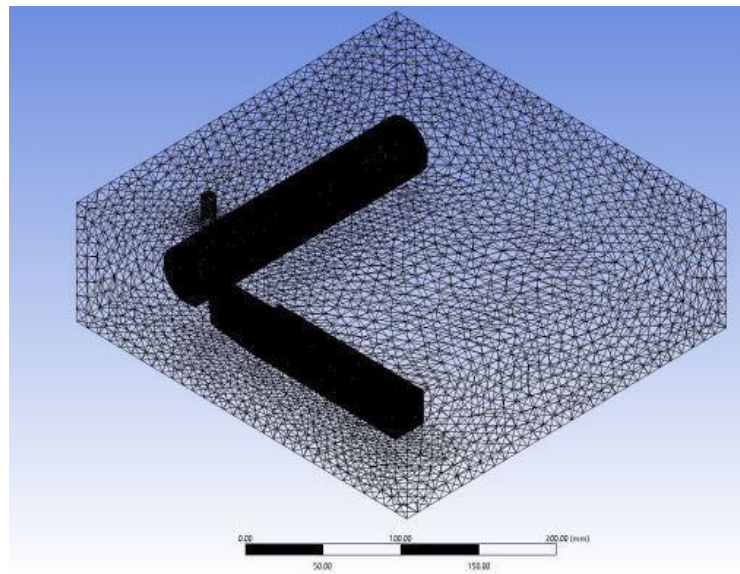
Figure.3 Coincided computational space with a lattice count of 5.90 million cells

3.3 Computational Liquid Elements Model

The issue is addressed utilizing a shaky, three-layered tempestuous incompressible stream. Because of conduction, temperature changes happen close to the apparatus and workpiece tip. Furthermore, the review centers around breaking down the convective intensity move coefficient, temperature, and Nusselt number. The Shear Pressure Transport thick model is utilized for this reason. Among the choppiness models regularly used to investigate violent streams, the k-ω SST model is outstanding.

3.3.1 Material Selection

Table 5 shows the warm properties of AISI 4130 Steel and M2 Molybdenum Rapid Apparatus Steel. The work piece material is AISI 4130 Steel, while UNS T11302 is utilized for the cutting instrument. The spout cross-segment is given a speed delta limit condition, permitting the Nanofluid to be showered on the work piece and cutting device. The Nano fluid's feedback speed is changed in strides of 5 m/s, going from 1 to 15 m/s. The essential goal is to explore what the Reynolds number means for different intensity move boundaries, including the convective intensity move coefficient and Nusselt number. Table 6 presents the underlying intensity hotspots for conduction, warming the slicing instrument tip to 1005.35 K and the work piece tip to 894.25K.

Table.5 Thermal characteristics of the tool for cutting and workpiece

Component	Thermal Conductivity (W/m-K)	Density (kg/m3)	Specific Heat (J/kg-K)
AISI 4130 Steel -Workpiece	45	7800	480

| (UNS T11302) - Cutting Tool	20	8260	470

<p align="center">Table.6 The maximum temperature reached through a cutting tool as well as workpiece</p>

Component	Kelvin
Temperature of Cutting Tool	1005.35
Temperature of Workpiece	894.25

3.4 Methods and Controls for Finding Solutions

The pressure-velocity relationship is circumvented by employing the SIMPLE approach. The equations for turbulent kinetic energy as well as momentum are solved using the second order upwind approach. The second-order upwind method is employed to solve both the energy problem and specific dissipation rates. For quicker convergence and more precise results, the under-relaxation variables are also changed. The residuals that remain for mass, momentum, energy, turbulent kinetic energy, and dissipation.

IV. RESULTS ANALYSIS
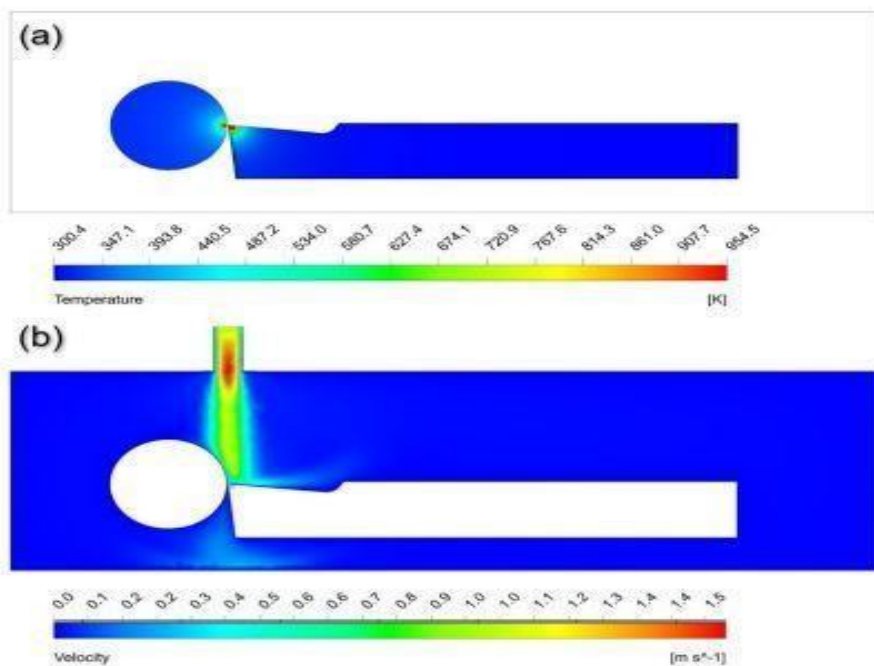
<p align="center">Figure.4 (a) Temperature dispersion on the cutting device and workpiece at a consistent state.</p>
<p align="center">(b) Speed forms in the computational area portraying the progression of nanofluid at the machining connection point.</p>

4.1. Impact of Nanoparticle Volume Part on Cutting Device Intensity Move Attributes

The investigation of intensity transmission and warm execution of Nanofluids for turning exercises is directed mathematically. To upgrade heat transmission, mineral oil is doped with nanoparticles to work on its warm attributes. At a consistent speed of one meter each second, the level of dissipated nanoparticles was changed, bringing about a Reynolds number of 55 and laminar stream. The volume division (F) of scattered nanoparticles in the slicing liquid reaches from 2% to 8%, as displayed in Tables 2-4, demonstrating an expansion in warm conductivity with a higher volume level of nanoparticles. Following the use of Nanofluids, an examination is led on the cutting device's greatest temperature in view of various nanoparticle types and explicit volume divisions, which change from 2% to 8%. Figure 5 outlines that an expansion in the volume part relates with a decline in the most extreme temperature.
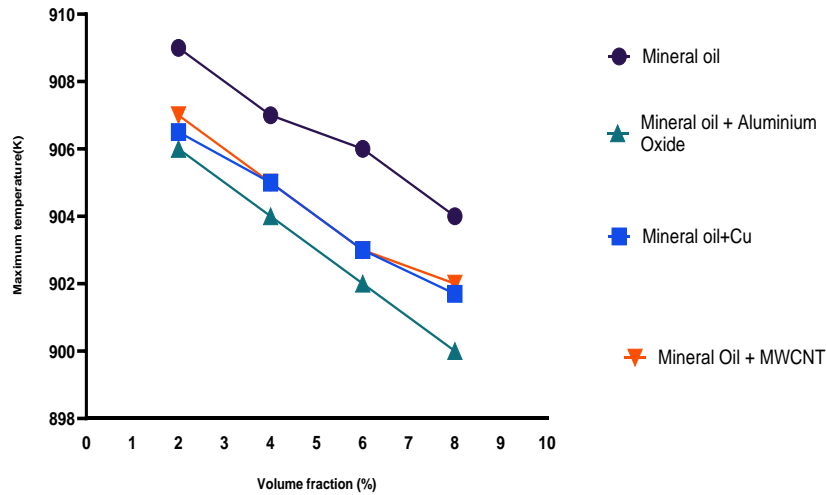
Figure 5. Variety in most extreme cutting apparatus temperature with various volume parts of scattered nanoparticles

The temperature slope alludes to the variety in temperature per unit length. It is a helpful measurement for surveying how temperature changes over a distance. Figure 6 delineates that the MWCNT-doped nanofluid shows the biggest temperature inclination for a volume portion of 2%. This distinction is featured by Table 1, which frames the thermophysical qualities of nanoparticles, demonstrating that MWCNT has a warm conductivity of 3000W/m-K, north of 30 times higher than that of Al_2O_3 and Cu. Thusly, the MWCNT-doped nanofluid displays a higher pace of intensity move. Besides, as the volume portion expands, the temperature distinction diminishes straightly. Figure.6 also, as the volume part expands the temperature angle uniqueness between Cu-Mineral Oil and Al_2O_3 - Mineral Oil nanofluids turns out to be more recognizable. In particular, at an 8% volume division, the Cu-Mineral Oil nanofluid has a temperature slope of 2,723,530 K/m, while theAl_2O_3- Mineral Oil nanofluid displays temperature angle of 2,776,830 K/m.
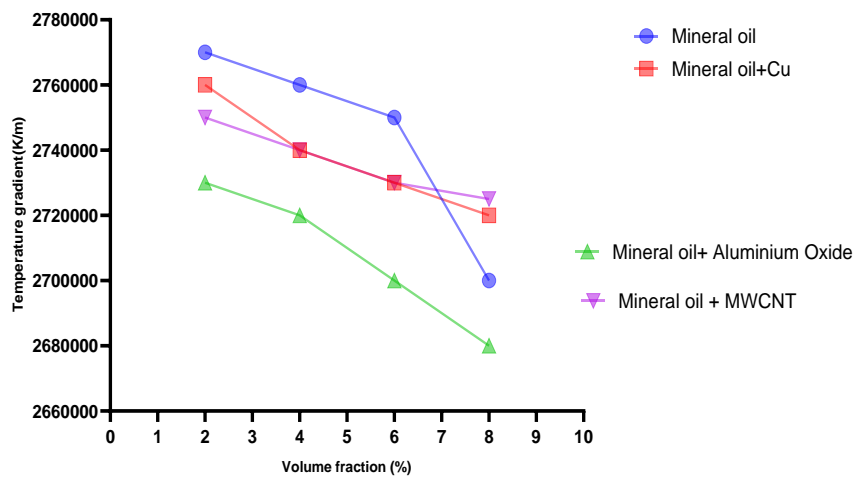

Figure.6 Variety in the temperature angle on the cutting apparatus with various volume parts of scattered nanoparticles

4.2 Impact of Nanoparticle Volume Division on Cutting Apparatus Intensity Move Attributes

The ongoing review explores the effect of nanofluid speed on the intensity source across a few factors, for example, the wall heat move coefficient, most extreme temperature, and temperature inclination. The critical intensity created from the slicing device's adherence to the chips prompts an extreme decrease in device life at higher temperatures. To resolve this issue, cutting liquid goes about as a coolant during the high velocity turning process, relieving miniature breaks, ductile remaining strains, and warm harm, hence keeping an optimal temperature. Curiously, the typical temperature diminishes as the volume rate increments. Furthermore, the stream happens in a laminar system with nanoparticles consistently scattered in the mineral oil at low Reynolds numbers, ordinarily under 200.Changing to higher Reynolds numbers moves the stream to a fierce system, bringing about very turbulent scattering and

Brownian movement of nanoparticles in the mineral oil. Temperature appropriation diminishes with Reynolds number, Figure 7 uncovers that rising Reynolds number upgrades inertial power.

Be that as it may, at higher Reynolds numbers, there's no critical fluctuation in temperature dissemination among various nanofluid arrangements. There view utilizes three particular nanoparticle types: Cu, Al_2O_3, and MWCNT, with cutting liquid velocities going from 1 m/s to 15 m/s. Figure 7 outlines the most extreme temperature as far as Reynolds number across these nanofluids at an 8% volume centralization of nanoparticles.
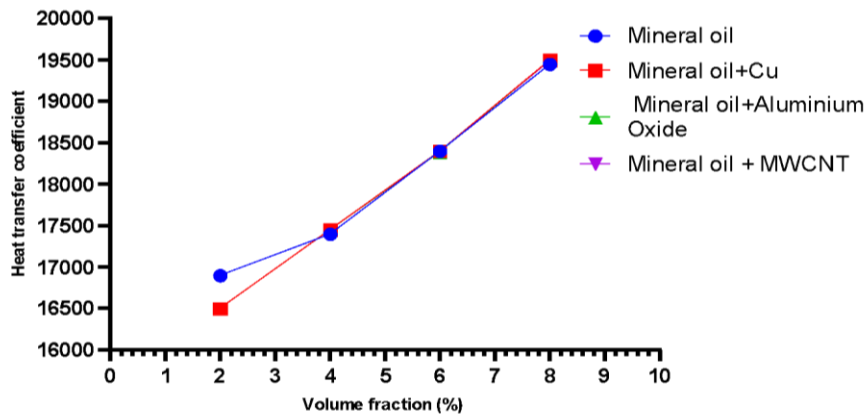

Figure.7 Variety in the convective intensity move coefficient of the cutting apparatus with various volume parts

As opposed to MWCNT and Cu nanofluids, Al_2O_3 shows lower temperatures across all volume portions going from 2% to 8%. A higher volume level of nanoparticles prompts a faster pace of intensity transmission, as demonstrated by the straight declining pattern displayed in Figure 7. Moreover, Al_2O_3 shows a quicker pace of temperature decline contrasted with other nanofluids. It is apparent that when nanoparticles are not consistently disseminated in the base liquid, the temperature at the contact point arrives at its greatest. A comparable discovery in regards to Al_2O_3 nanofluids presentation has been recorded in the writing .The variety in temperature per unit length is named the temperature slope. One helpful measurement for evaluating how temperature changes over a distance is the temperature slope. As portrayed in Figure7, the MWCNT-doped nanofluid shows the biggest temperature slope for a volume portion of 2%. It is obvious from Table 1, enumerating the thermophysical qualities of nanoparticles, that MWCNT has a warm conductivity of 3000 W/m-K, which is north of 30 times higher than that of Al_2O_3 and Cu. Accordingly, for MWCNT-doped nanofluid, the intensity move rate is higher. In addition, as the volume portion expands, the temperature angle diminishes straightly.

4.3 Impact of Reynolds Number on Cutting Device Intensity Move Qualities

The ongoing review explores the effect of nanofluid speed on the intensity source across a few factors, for example, the wall heat move coefficient, most extreme temperature, and temperature inclination. The critical intensity created from the slicing device's adherence to the chips prompts an extreme decrease in device life at higher temperatures. To resolve this issue, cutting liquid goes about as a coolant during the high velocity turning process, relieving miniature breaks, ductile remaining strains, and warm harm, hence keeping an optimal temperature. Curiously, the typical temperature diminishes as the volume rate increments. Furthermore, the stream happens in a laminar system with nanoparticles consistently scattered in the mineral oil at low Reynolds numbers, ordinarily under 200. Changing to higher Reynolds numbers moves the stream to a fierce system, bringing about very turbulent scattering and Brownian movement of nanoparticles in the mineral oil. Albeit the temperature appropriation diminishes with Reynolds number, Figure 8 uncovers that rising Reynolds number upgrades inertial power. Be that as it may, at higher Reynolds numbers, there's no critical fluctuation in temperature dissemination among various nanofluid arrangements. The review utilizes three particular nanoparticle types: Cu, Al_2O_3 and MWCNT, with cutting liquid velocities going from 1 m/s to 15 m/s. Figure 8 outlines the most extreme temperature as far as Reynolds number across these nanofluids at a 8% volume centralization of nanoparticles.
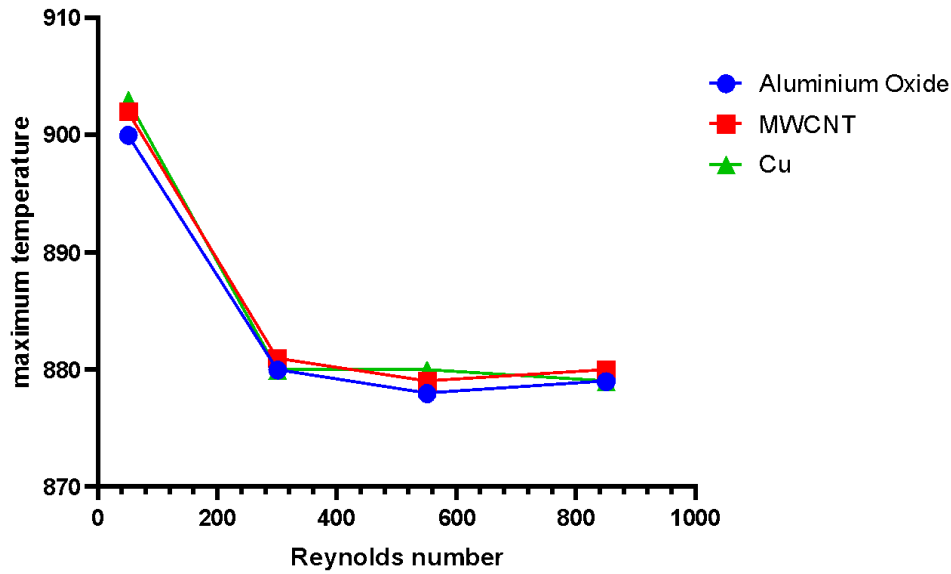
Figure.8 Variety in greatest slicing apparatus temperature as for Reynolds number

The convective heat transfer coefficient plays a vital role in analyzing the thermal performance of nanofluids as cutting fluids. Figure 9 depicts the convective heat transfer coefficient at various velocities. Figure 9 demonstrates how the convective heat transfer coefficient increases with the rise in nanofluid velocity. Moreover, as the volume percentage of nanoparticles increases, both the Nusselt number and convective heat transfer coefficient also increase. In Figure 9, it is evident that MWCNT nanofluid exhibits a higher convective heat transfer coefficient compared to Cu and Al_2O_3. This remains valid for lower Reynolds numbers, ranging between 55 and 432. On the contrary, for Reynolds numbers exceeding 432, Al_2O_3 shows the highest convective heat transfer coefficient when compared to Cu and MWCNT. Consequently, we can conclude that for Reynolds numbers higher than 432, Al_2O_3 demonstrates a stronger convective heat transfer coefficient, while MWCNT displays superior heat transfer qualities at lower Reynolds numbers.
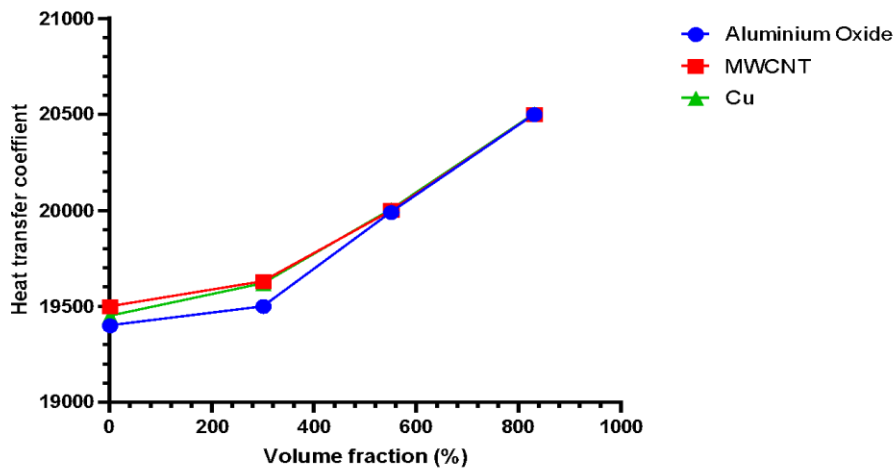

Figure.9 Variety in convective intensity move coefficient of the slicing apparatus concerning Reynolds number.

One more fundamental measurement for evaluating the warm proficiency of a particular nanofluid is the Nusselt number, which implies the proportion of convective intensity move to conductive intensity move at a liquid limit. Figure 10 portrays the variety of the Nusselt number among various nanofluids concerning the Reynolds number. The chart explains that with an expansion in the Reynolds number, the Nusselt number additionally increments for each nanofluid. Besides, past a Reynolds number of 600, the Nusselt number raises all the more steeply. Dissipated Al_2O_3 nanofluids show better warm execution analyzed than scattered Cu and MWCNT nanofluids.
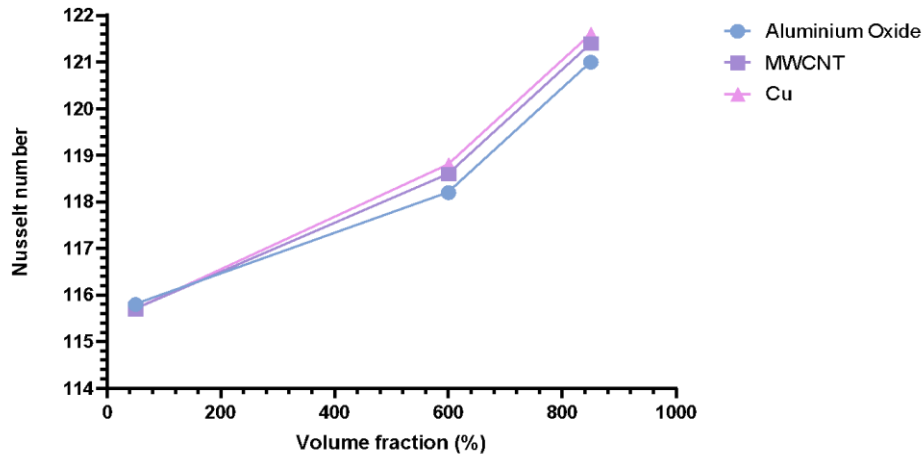
Figure.10 Variety in Nusselt number as for Reynolds number

V. CONCLUSIONS

This study looks at the temperature conveyance on the outer layer of a cutting device and workpiece during turning tasks utilizing different nanocoolants, broke down mathematically with Computational Liquid Elements (CFD). The computational space incorporates a hot workpiece and instrument, and a spout over the machining zone is utilized to splash nanocoolants. Mineral oil scatters nanoparticles of copper, aluminum dioxide, and multi-walled carbon nanotubes at various volume portion rates. By changing the coolant speed (Uc) and nanoparticle volume portion (F), the intensity move abilities of a few nanocoolants are assessed. Different attributes, for example, most extreme apparatus temperature, cutting instrument temperature inclination, convective intensity move coefficient and Nusselt number are analyzed across various volume rates and Reynolds numbers. The discoveries propose that nanofluids with higher warm conductivity and lower explicit intensity limit will show worked on warm execution. The ends from this examination are summed up underneath:

An expansion in the volume level of scattered nanoparticles brings about a direct lessening in the cutting device and workpiece temperature. This happens in light of the fact that a higher volume division decreases temperature, improving the thermophoresis and Brownian movement of nanoparticles. The relationship between's machining temperature and Reynolds number shows a lessening. As the Reynolds number builds, the temperature inside the machining zone diminishes because of the expanded inertial power of the nanocoolants. When the molecule volume part is expanded from 2% to 8%, mineral oil blended in with MWCNT nanoparticles higher convective intensity move coefficient. Furthermore, contrasted with different sets of nanocoolants, MWCNT nanocoolants show the best temperature decrease per unit length with an expansion in molecule volume part. Both the Nusselt number and convective intensity move coefficient of nanocoolants increment with Reynolds number. Expanded inertial powers speed up constrained convection heat rates in the machining zone, prompting this impact.This concentrate plainly shows that for turning tasks, MWCNT nanocoolants are better due than their higher constrained convective intensity move rate and temperature decrease in the machining zone contrasted with Cu and Al₂O₃ nanocoolants, featuring their excellent warm presentation.

REFERENCES

[1] Anandan, V., Babu, M. N., Sezhian, M. V., Yildirim, C. V., & Babu, M. D. (2021). Influence of graphene nanofluid on various environmental factors during turning of M42 steel. *Journal of Manufacturing Processes*, *68*, 90–103. https://doi.org/10.1016/j.jmapro.2021.07.019

[2] Pal, A., Chatha, S. S., & Sidhu, H. S. (2021). Performance evaluation of the minimum quantity lubrication with Al2O3-mixed vegetable-oil-based cutting fluid in drilling of AISI 321 stainless steel. *Journal of Manufacturing Processes*, *66*, 238–249. https://doi.org/10.1016/j.jmapro.2021.04.024

[3] Srikant, R., Prasad, M., Amrita, M., Sitaramaraju, A., & Krishna, P. V. (2013). Nanofluids as a potential solution for Minimum Quantity Lubrication: A review. *Proceedings of the Institution of Mechanical Engineers. Part B, Journal of Engineering Manufacture*, *228*(1), 3–20. https://doi.org/10.1177/0954405413497939

[4] 4. Das, A., Pradhan, O., Patel, S. K., Das, S. R., & Biswal, B. B. (2019). Performance appraisal of various nanofluids during hard machining of AISI 4340 steel. *Journal of Manufacturing Processes*, *46*, 248–270. https://doi.org/10.1016/j.jmapro.2019.07.023

[5]   Kumar, A., Ghosh, S., & Aravindan, S. (2019). Experimental investigations on surface grinding of silicon nitride subjected to mono and hybrid nanofluids. *Ceramics International*, *45*(14), 17447–17466. https://doi.org/10.1016/j.ceramint.2019.05.307

[6]   Das, A., Pradhan, O., Patel, S. K., Das, S. R., & Biswal, B. B. (2019). Performance appraisal of various nanofluids during hard machining of AISI 4340 steel. *Journal of Manufacturing Processes*, *46*, 248–270. https://doi.org/10.1016/j.jmapro.2019.07.023

[7]   Fang, Z., & Obikawa, T. (2020). Influence of cutting fluid flow on tool wear in high-pressure coolant turning using a novel internally cooled insert. *Journal of Manufacturing Processes*, *56*, 1114–1125. https://doi.org/10.1016/j.jmapro.2020.05.028

[8]   Jerold, B. D., & Kumar, M. P. (2011). Experimental investigation of turning AISI 1045 steel using cryogenic carbon dioxide as the cutting fluid. *Journal of Manufacturing Processes*, *13*(2), 113–119. https://doi.org/10.1016/j.jmapro.2011.02.001

[9]   Zhang, Y., Li, C., Jia, D., Zhang, D., & Zhang, X. (2015b). Experimental evaluation of the lubrication performance of MoS2/CNT nanofluid for minimal quantity lubrication in Ni-based alloy grinding. *International Journal of Machine Tools & Manufacture/International Journal of Machine Tools and Manufacture*, *99*, 19–33. https://doi.org/10.1016/j.ijmachtools.2015.09.003

[10]   Mahmud, S. A., Ismail, A. F., Bappy, J. H., & Noor, W. I. (2023). A study on Accuracy range of multiphase mixture model for turbulent convective heat transfer Enhancement Simulation of Water-AL2O3 nanofluid. *Journal of Nanofluids*, *12*(2), 438–447. https://doi.org/10.1166/jon.2023.1972

[11]   Zhang, Y., Li, C., Jia, D., Zhang, D., & Zhang, X. (2015). Experimental evaluation of MoS2 nanoparticles in jet MQL grinding with different types of vegetable oil as base oil. *Journal of Cleaner Production*, *87*, 930–940. https://doi.org/10.1016/j.jclepro.2014.10.027

[12]   Srikant, R., & Ramana, V. (2015). Performance evaluation of vegetable emulsifier based green cutting fluid in turning of American Iron and Steel Institute (AISI) 1040 steel – an initiative towards sustainable manufacturing. *Journal of Cleaner Production*, *108*, 104–109. https://doi.org/10.1016/j.jclepro.2015.07.031

[13]   Duc, T. M., Long, T., & Chien, T. Q. (2019). Performance evaluation of MQL parameters using AL2O3 and MOS2 nanofluids in hard turning 90CRSI steel. *Lubricants*, *7*(5), 40. https://doi.org/10.3390/lubricants7050040

[14]   Gugulothu, S., & Pasam, V. K. (2020). Experimental investigation to study the performance of CNT/MoS2 hybrid nanofluid in turning of AISI 1040 stee. *Australian Journal of Mechanical Engineering*, *20*(3), 814–824. https://doi.org/10.1080/14484846.2020.1756067

[15]   Jia, D., Li, C., Zhang, D., Zhang, Y., & Zhang, X. (2014). Experimental verification of nanoparticle jet minimum quantity lubrication effectiveness in grinding. *Journal of Nanoparticle Research*, *16*(12). https://doi.org/10.1007/s11051-014-2758-7

[16]   Setti, D., Sinha, M. K., Ghosh, S., & Rao, P. V. (2015). Performance evaluation of Ti–6Al–4V grinding using chip formation and coefficient of friction under the influence of nanofluids. *International Journal of Machine Tools & Manufacture/International Journal of Machine Tools and Manufacture*, *88*, 237–248. https://doi.org/10.1016/j.ijmachtools.2014.10.005

[17]   17. Zhang, X., Li, C., Zhang, Y., Wang, Y., Li, B., Yang, M., Guo, S., Liu, G., & Zhang, N. (2017). Lubricating property of MQL grinding of Al2O3/SiC mixed nanofluid with different particle sizes and microtopography analysis by cross-correlation. *Precision Engineering*, *47*, 532–545. https://doi.org/10.1016/j.precisioneng.2016.09.016

[18]   18. Shuang, Y., John, M., & Songlin, D. (2019b). Experimental investigation on the performance and mechanism of graphene oxide nanofluids in turning Ti-6Al-4V. *Journal of Manufacturing Processes*, *43*, 164–174. https://doi.org/10.1016/j.jmapro.2019.05.005

[19]   Singh, H., Sharma, V. S., Singh, S., & Dogra, M. (2019). Nanofluids assisted environmental friendly lubricating strategies for the surface grinding of titanium alloy: Ti6Al4V-ELI. *Journal of Manufacturing Processes*, *39*, 241–249. https://doi.org/10.1016/j.jmapro.2019.02.004

[20]   Fang, Z., & Obikawa, T. (2020). Influence of cutting fluid flow on tool wear in high-pressure coolant turning using a novel internally cooled insert. *Journal of Manufacturing Processes*, *56*, 1114–1125. https://doi.org/10.1016/j.jmapro.2020.05.028

[21]   Gariani, S., Shyha, I., Inam, F., & Huo, D. (2017). Evaluation of a novel controlled cutting fluid impinging supply system when machining titanium alloys. *Applied Sciences*, *7*(6), 560. https://doi.org/10.3390/app7060560

[22]   Shuang, Y., John, M., & Songlin, D. (2019). Experimental investigation on the performance and mechanism of graphene oxide nanofluids in turning Ti-6Al-4V. *Journal of Manufacturing Processes*, *43*, 164–174.

https://doi.org/10.1016/j.jmapro.
2019.05.005

[23]   El-Bouri, W., Deiab, I., Khanafer, K., & Wahba, E. (2019). Numerical and experimental analysis of turbulent flow and heat transfer of minimum quantity lubrication in a turning process using discrete phase model. *International Communications in Heat and Mass Transfer*, *104*, 23–32. https://doi.org/10.1016/j.icheatmasstransfer.2019.02.012

[24]   Zenjanab, M. J., Pedrammehr, S., Qazani, M. R. C., & Shabgard, M. R. (2021). Influence of Cutting Fluid-Based CuO-Nanofluid with Boric Acid-Nanoparticles Additives on Machining Performances of AISI 4340 Tool Steel in High-Speed Turning Operation. *Mechanical & Materials Engineering/Iranian Journal of Science and Technology. Transactions of Mechanical Engineering*, *46*(2), 335–345. https://doi.org/10.1007/s40997-021-00452-2

[25]   Sharma, A. K., Tiwari, A. K., & Dixit, A. R. (2018). Prediction of temperature distribution over cutting tool with alumina-MWCNT hybrid nanofluid using computational fluid dynamics (CFD) analysis. ˜ *the œ International Journal of Advanced Manufacturing Technology/International Journal, Advanced Manufacturing Technology*, *97*(1–4), 427–439. https://doi.org/10.
1007/s00170-018-1946-5